Applied Thermal Engineering 31 (2011) 1141–1149

Contents lists available at ScienceDirect

Applied Thermal Engineering

journal homepage: www.elsevier.com/locate/apthermeng

Configuration optimization of regularly spaced short-length twisted tape in a circular tube to enhance turbulent heat transfer using CFD modeling

Yangjun Wang [a], Meiling Hou [a], Xianhe Deng [b], Li Li [a], Cheng Huang [c], Haiying Huang [c], Gangfeng Zhang [c], Changhong Chen [c,*], Weijun Huang [d]

[a] School of Environmental and Chemical Engineering, Shanghai University, Shanghai 200444, PR China
[b] Institute of Chemical Engineering, South China University of Technology, Guangzhou 510640, PR China
[c] Shanghai Academy of Environmental Sciences, Shanghai 200233, PR China
[d] School of Mechanical and Automotive Engineering, South China University of Technology, Guangzhou 510640, PR China

ARTICLE INFO

Article history:
Received 21 July 2010
Accepted 3 December 2010
Available online 21 December 2010

Keywords:
Configuration optimization
Short-length twisted tape
Heat transfer Enhancement
Computational fluid dynamics (CFD)

ABSTRACT

This work presents the configuration optimization of regularly spaced short-length twisted tape in a circular tube for turbulent heat transfer in air using computational fluid dynamics (CFD) modeling. The configuration parameters include the free space ratio (s), twist ratio (y) and rotated angle (α). The computational results are in good agreement with experimental data. The results indicate that the larger rotated angle yields a higher heat transfer value and a greater flow resistance, whereas the smaller twist ratio results in better heat transfer performance using a twist ratio ranging from 2.5 to 8.0 except for a large rotated angle and a high Reynolds number (e.g., $\alpha = 360^\circ$ and Re = 20,200). However, the minimum resistance factor occurs if the twist ratio is in the range of 4.75–5.75. The optimal design of regularly spaced short-length twisted tape in a circular tube for turbulent air flow is $y = 4.25$–4.75, $\alpha = 180^\circ$ and $s = 28$–33 with a Reynolds number that varies from 10,000 to 20,200. If the heat transfer rate is more important, the second design of $y = 4.25$–4.75, $\alpha = 270^\circ$ and $s = 28$–33 in the range of Reynolds numbers from 10,000 to 20,200 can be used as a reference for industrial application.

1. Introduction

Heat exchangers are widely used in various areas such as power production, chemical and food industries, environmental engineering, waste heat recovery, the manufacturing industry, air conditioning, refrigeration and space applications. Heat enhancement technology plays an important role in conserving energy and protecting the environment. Single-phase heat transfer can be increased using artificially roughened surfaces and other augmentation techniques such as vortex generators and modifications to duct cross-sections and surfaces [1]. These augmentation techniques belong to the passive category, which can increase the convective heat transfer coefficient on the tube side. Among the many techniques investigated for the augmentation of heat transfer rates inside of round tubes, a wide range of inserts, such as tapered spiral inserts, packings, rings, disks, streamlined shapes, mesh inserts, spiral brush inserts [2], conical-nozzles [3] and V-nozzles [4], have been used to minimize the size of heat exchangers and thus reduce the capital investments for a given load.

The insertion of twisted tape into a tube is an attractive method to improve the convective heat transfer coefficient in existing systems because it generates a swirl flow, which can induce a tangential flow velocity component and enhance fluid mixing between the duct core and the near-wall region. However, most studies have focused on viscous liquid or laminar flow [5,6,7] because twisted tape generates a larger increase in the pressure drop for turbulent flow than that of laminar flow compared to the absence of twisted tape in the tube. Manglik and Bergles [8] and Sarma et al. [9] developed thermal-hydraulic correlations for heat transfer and pressure drop for in-tube turbulent flows with twisted tape inserts. Although the heat transfer was enhanced, the pressure drop increased considerably for turbulent flow ($5{,}000 < \mathrm{Re} < 25{,}000$) in the tube fitted with modified full-length twisted tape (serrated twisted tape) [10]. For turbulent flow, the heat transfer augmentation by traditional full-length twisted tape is typically not satisfied due to a considerable increase in the pressure drop for industrial applications.

The short-length twisted tape can increase the heat transfer coefficient in the tube by generating a swirl flow too, although the

* Corresponding author. Tel./fax: +86 21 64085119.
E-mail address: chench@saes.sh.cn (C. Chen).

1359-4311/$ – see front matter © 2010 Elsevier Ltd. All rights reserved.
doi:10.1016/j.applthermaleng.2010.12.009

swirl flow gradually decays downstream between the short-length twisted tapes. The most attractive advantage is that the flow resistance in the free space (the section without short-length twisted tape) is lower than that with full-length twisted tape. This effective heat transfer enhancement technology has attracted the interest of researchers. Saha et al. [11] investigated the heat transfer and pressure drop characteristics of laminar flow in a tube fitted with regularly spaced twisted-tape elements. Effects of the Reynolds number, Prandtl number, twist ratio, space ratio, and rod-to-tube diameter ratio on heat transfer rate were also reported. Date and Gaitonde [12] introduced the correlations for predicting characteristics of laminar flow in a tube fitted with regularly spaced twisted tape elements. Date and Saha [13] numerically predicted the friction and the heat transfer characteristics for laminar flow in a round tube fitted with regularly spaced twisted-tape elements that are connected by thin round rods and reported the considerably enhanced thermo hydraulic performance was achievable by increasing the number of turns on the tape elements, by reducing the connecting rod diameter, and at high fluid Prandtl numbers. Saha et al. [14] reported the effect of Reynolds number, Prandtl number, twist ratio, space ratio, tape-width, rod-diameter and phase angle between consecutive tape elements on heat transfer and pressure drop characteristics in a round tube fitted with regularly spaced twisted-tape elements for laminar swirl flow of a viscous fluid having intermediate Prandtl number range (205–518).

But only a few studies have been performed regarding turbulent flow. Eiamsa-ard et al. [15] studied the enhancement efficiency of the tube with only a single short-length tape insert; however, its enhancement efficiency was lower than that with the full-length insert for Reynolds numbers in a range from 4,000 to 20,000. Especially for a Reynolds number in the range of 10,000–20,000, the enhancement efficiencies were all lower than 1.0, which means the heat transfer enhancement is not satisfied.

Studies related to regularly spaced short-length twisted tape in tubes for turbulent flow are limited. Eiamsa-ard et al. [16] experimentally studied the heat transfer and friction factor in a double-pipe heat exchanger fitted with regularly spaced twisted-tape elements. Two different cases were reported in their study: (1) full-length typical twisted tape at different twist ratios ($y = 6.0$ and 8.0), and (2) twisted tape with various free space ratios ($s = 1.0$, 2.0, and 3.0). The experimental results demonstrated that different types of twisted-tape constructions in the inner tube of a double-pipe heat exchanger effectively improved the heat transfer rate; however, the friction factor of the tube also increased considerably. Furthermore, the enhancement efficiency which can be calculated from their data was much less than 1.0 for a Reynolds number in the range of 2,000–12,000 which can be primarily attributed to the experimental configuration parameters.

The heat transfer and flow resistance characteristics of short-length twisted tape regularly spaced in a tube are significantly impacted by the configuration parameters. Additionally, the most important parameter for heat exchanger design is the heat transfer enhancement efficiency (η). Thus, the determination of the optimal configuration parameters of regularly spaced short-length twisted tape in a tube is essential for the sake of attaining the maximum heat transfer enhancement efficiency for turbulent flow. However, no such study has been reported in the available literature. In this paper, the heat transfer and friction factor characteristics in a plain circular tube with regularly spaced short-length twisted tape for Reynolds numbers in the range of 10,000–20,200 were investigated, and the configuration optimization was performed based on the heat transfer enhancement efficiency using computational fluid dynamics (CFD) modeling for a wide range of twist ratios, rotated angles, and free space ratios.

2. Numerical simulation

2.1. Problem formulation

The heat transfer and flow resistance of regularly spaced short-length twisted tape in round tubes are affected by the configuration parameters for turbulent air flow. A layout of a round tube with regularly spaced short-length twisted tape is shown in Fig. 1. The internal tube diameter is 16 mm ($d_i = 16$ mm), and the twisted-tape thickness is 1.2 mm ($\delta = 1.2$ mm). Three parameters were selected as independent parameters: 1) twist ratio (y); 2) rotated angle (α); 3) free space ratio (s). Here,

$$l = H\cdot\alpha/180 \tag{1}$$

$$y = H/d_i \tag{2}$$

$$s = l_p/d_i - y\cdot\alpha/180 \tag{3}$$

After the air passes the tube, the swirl flow is generated by the short-length twisted tape, decays in the free space between the tape elements and is augmented by the short-length of the twisted tape that follows; thus, periodic flow is established. In this paper, an investigation of heat transfer and flow resistance for fully developed periodic flow is performed. The computational domain and Cartesian coordinate system are shown in Fig. 2.

2.2. Numerical methods

A three-dimensional numerical simulation of the heat transfer and flow resistance was conducted using the FLUENT 6.1 CFD code. The model was used to optimize the configuration parameters of regularly spaced short-length twisted tape in a tube for 3-D, steady, incompressible air periodic flow with constant properties. The CFD model involves numerical solutions of the conservation equations for mass, momentum and energy. These equations can be written for incompressible flows as follows:

Mass conservation:

$$\frac{\partial\rho}{\partial t} + \nabla\cdot(\rho\vec{u}) = 0 \tag{4}$$

Momentum conservation:

$$\frac{\partial(\rho\vec{u})}{\partial t} + \nabla\cdot(\rho\vec{u}\vec{u}) = \rho g - \nabla P + \nabla\cdot(\bar{\bar{\tau}}) \tag{5}$$

Energy conservation:

$$\frac{\partial(\rho e)}{\partial t} + \nabla\cdot(\vec{u}(\rho e + P)) = \nabla\cdot\left(K_{eff}\nabla T + \left(\bar{\bar{\tau}}_{eff}\cdot\vec{u}\right)\right) \tag{6}$$

Here,

$$\bar{\bar{\tau}}_{eff} = \mu\left(\left(\nabla\vec{u} + \nabla\vec{u}^T\right) - \frac{2}{3}\nabla\cdot\vec{u}t\right) \tag{7}$$

The convective term was discretized using the QUICK scheme, and the linkage between the velocity and pressure was computed using the SIMPLEC algorithm. The Enhanced Wall Treatment model was

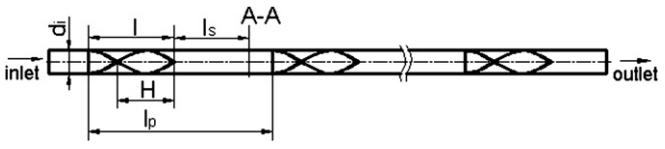

Fig. 1. Layout of a round tube with regularly spaced short-length twisted tape.

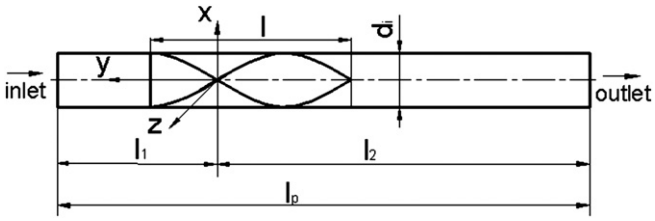

Fig. 2. Scheme of the computational domain.

chosen for the near-wall modeling method because it combines the use of a blended law-of-the-wall and a two-layer zonal model and generally requires a fine near-wall mesh that is capable of resolving the viscous sub-layer. In this study, the realizable k–ϵ model [17] was used to model the turbulent flow regime. The mesh independency was tested for these three grids. For the case of $y = 4.25$, $\alpha = 270^\circ$ and $l_p = 600$ mm, the computational grid includes 436,360 cells. The mesh dependency was examined by solving the flow field for three mesh configurations made of 232,540, 333,632, and 436,360 cells, respectively, and we compared the Nusselt numbers and flow resistance factors for the three mesh configurations respectively. Results showed that up to 1.97% and 1.27% difference of the Nusselt number and flow resistance factor respectively existed between the coarser and finer mesh and less than 0.196% and 0.212% difference existed between the two finer meshes, which indicated that the finer mesh resulted in mesh-independent solutions. In the same way, three grids were used to examine the mesh independence for every case. At last, the simulation grid in this study was meshed using GAMBIT 2.1 with about from 400,000 to 450,000 cells that consisted of tetrahedrons and hexahedrons, depending on the different layouts. Fig. 3 shows an example of the partial meshed configuration of the round tube equipped regularly with short-length twisted tape. In addition, a convergence criterion of 10^{-6} was used for all of the calculated parameters.

2.3. Boundary conditions

The air inlet temperature was specified as 300 K, and three assumptions were made in the model: (1) the temperature of the tube wall was constant ($T_w = 400$ K); (2) the wall of the short-length twisted tape was adiabatic; and (3) the physical properties of air were constant and were evaluated at the bulk temperature. The periodic boundary condition was adopted at the inlet and outlet of the domain shown in Fig. 2 with respect to the main flow direction.

3. Experimental setup

Before the simulation of the configuration optimization is performed, the reliability of the simulation method should be confirmed. For this purpose, the experimental investigation is included in this paper. A schematic diagram of the experimental heat exchanger system is shown in Fig. 4. The experiments were performed in a double-pipe heat exchanger with both ends assembled with a sealing gasket to ensure a good seal. Initially, air entered the inner tube from a flexible centrifugal blower. A rotameter was used to measure the air flow rate. A data logger (Agilent HP3470A) was used to record the temperatures that were measured by copper-constantan thermocouples. The pressure drop of the air flow was measured with U-tube manometers where water was taken as the manometer fluid. The test tube was heated by steam in the outside tube from an electrically heated boiler, which provided a constant temperature boundary condition for the outside wall. The test section, inlet section, outlet section and stream tube were all insulated with a layer of glass wool. In the outlet section, there were four stations located in the same transverse section to measure the outlet bulk temperature. The distances to the inside wall were determined and set for the four stations. The average temperature of the four stations was considered as the outlet bulk temperature of the air. The bulk temperature of the air at the inlet was measured with a thermocouple positioned in the downstream of the short-length twisted tape, which was located in the upstream of the test section. At the upstream of test pipe, air passed a stabilizer, which included a conical diffuser, a fluid straightener and wire mesh screens to eliminate the effect of the curved pipe section after the centrifugal blower. Subsequently, air passed a short-length twisted tape, which was same to those mounted in the test section. As a result, the air flow was directed into the decaying swirl flow in the beginning of flow in the test section, which caused the flow in the test section to be similar to periodical flow. The short-length twisted tape was made of stainless steel strips with a thickness (δ) of 1.2 mm, and its width was close to the internal tube diameter. It was fabricated by twisting a straight tape about its longitudinal axis while it was held under tension. Each short-length twisted tape had two pores at both ends along its longitudinal axis. Before being inserted in the test tube, the short-length twisted tape was linked by slender constantan wires that were inserted into the pores. The plain test tube was a commercial copper tube with dimensions of $\phi 19 \times 1.5$ ($d_o = 19$ mm, $d_i = 16$ mm). The length of the test section, inlet section and outlet section was equal to 2100 mm, 200 mm and 200 mm respectively.

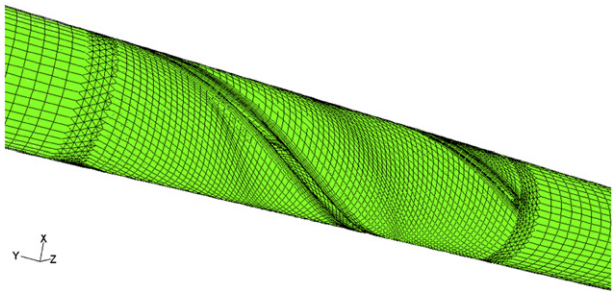

Fig. 3. Partial view of the meshing scheme.

4. Data reduction

The mean Nusselt number and the flow resistance factor were based on the inside diameter of the plain tube, and heat was transferred from the steam in the annulus side to the air in the inner tube. The heat transfer rate can be written as:

$$Q = \dot{m} \cdot C_p \cdot (t_{aout} - t_{ain}) \tag{8}$$

Here,

$$\dot{m} = V \cdot \rho / 360 \tag{9}$$

The mean velocity of air can be expressed as:

$$U = \frac{\dot{m}}{\frac{\pi}{4} d_i^2 \cdot \rho} \tag{10}$$

The Reynolds number can be written as:

$$\mathrm{Re} = \frac{d_i U \rho}{\mu} \tag{11}$$

The overall heat transfer coefficient can be written as:

$$K = \frac{Q}{\pi \cdot d_o \cdot l_{\exp} \cdot \Delta t_m} \tag{12}$$

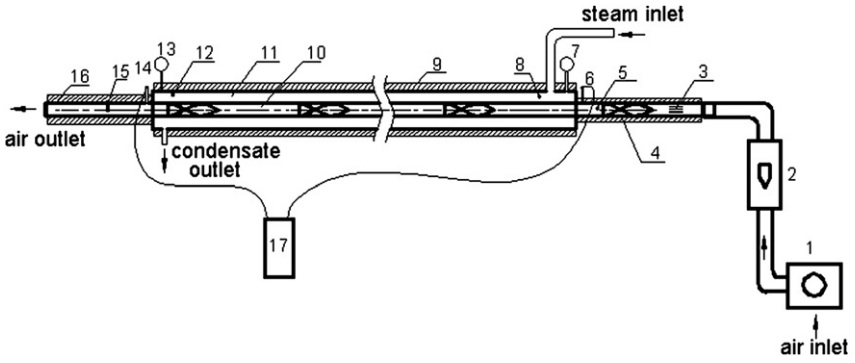

Fig. 4. Schematic diagram of the experimental setup. 1. Centrifugal blower; 2. Rotameter; 3. Stabilizer; 4. Layer of glass wool insulation in the air inlet section; 5. Inlet air bulk temperature measuring station; 6. Air pressure drop measuring station in the inlet section; 7. Pressure-measuring station in the inlet steam; 8. Temperature-measuring station in the inlet steam; 9. Layer of glass wool insulation in the test section; 10. Test tube; 11. Annulus side; 12. Temperature-measuring station in the outlet steam; 13. Pressure-measuring station in the outlet steam; 14. Air pressure drop measuring station in the outlet section; 15. Outlet air bulk temperature measuring station; 16. Layer of glass wool insulation in the air outlet section; 17. U-tube manometers.

The logarithmic mean temperature difference can be written as:

$$\Delta t_m = \frac{t_{aout} - t_{ain}}{\ln\left(\frac{t_{steam}-t_{ain}}{t_{steam}-t_{aout}}\right)} \tag{13}$$

Before the tube-side heat transfer coefficient was determined, the thermal resistances of the copper-tube wall and outside of the tube were estimated.

The thermal resistance of the outside of the tube [18] was determined from

$$R_o = 1/h_o \tag{14}$$

The temperature of the outside of the tube was assumed to be 100 °C, and the absolute pressure of the steam was specified as 0.2 MPa, thus,

$$R_o = 3.5162 \times 10^{-4}\mathrm{m^2K\cdot J^{-1}}$$

The thermal resistance of the copper-tube wall was calculated from

$$R_w = \frac{d_o}{2\cdot\lambda_w}\cdot\ln\left(\frac{d_o}{d_i}\right) \tag{15}$$

$$R_w = 1.4978 \times 10^{-5}\mathrm{m^2K\cdot J^{-1}}$$

The thermal resistance of the inside of the tube was estimated from

$$R_i = \frac{1}{h_i}\cdot\frac{d_o}{d_i} \tag{16}$$

By assuming that the Reynolds number of air in the tube is 20,000, and using the Dittus–Boelter equation for heat transfer, then

$$R_i = 0.0122\mathrm{m^2K\cdot J^{-1}}$$

Thus,

$$R_o/R_i = 0.0288 \quad \text{and} \quad R_w/R_i = 0.0012$$

The thermal resistance of the outside of the tube was only 0.0288 times as large as that of the inside of the tube, and the thermal resistance of the copper-tube wall was only 0.0012 times as large as that of the inside of the tube. Therefore, the thermal resistances of both the copper-tube wall and the outside of the tube were very small, and their change with the air flow rate could be neglected for this experimental study. Then, the tube-side heat transfer coefficient h_i was calculated from

$$\frac{1}{K} = \frac{1}{h_i}\cdot\frac{d_o}{d_i} + R_o + R_w \tag{17}$$

Thus,

$$\mathrm{Nu} = \frac{h_i\cdot d_i}{\lambda} \tag{18}$$

The flow resistance factor of air was estimated using

$$f = \frac{\Delta P}{\left(\frac{l_{exp}}{d_i}\right)\cdot\left(\frac{\rho\cdot u^2}{2}\right)} \tag{19}$$

5. Results and discussion

5.1. Validation

5.1.1. Validation using the published correlations

The experimental results of the plain tube without a twisted tape insert were first validated with previously published correlations to perform an evaluation of the error. The Nusselt number (Nu) and friction factor (f) were confirmed with previous correlations [19]. The Dittus–Boelter equation (or Gnielinski equation) for heat transfer and the Petukhov equation (or Blasius equation) for the friction factor are depicted in Fig. 5. The results of the plain tube from the present work are in good agreement with those of previous studies and are within ±8.06% deviation for the heat transfer (Nu) and ±5.29% for the friction factor (f). The results of the present work

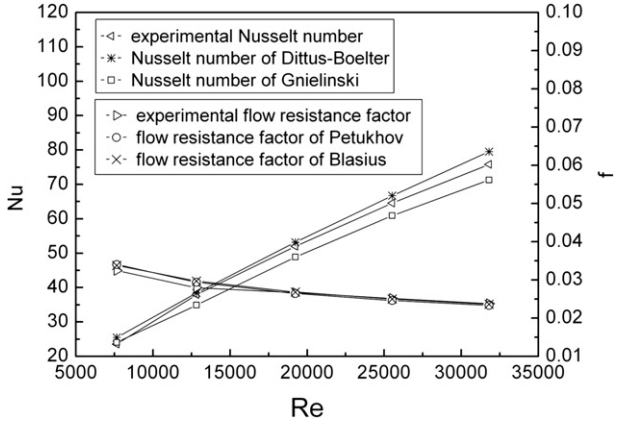

Fig. 5. Verification of experimental data of the plain tube.

of the plain tube are correlated as shown in Equations (20) and (21) for the Nusselt number and friction factor, respectively.

$$\mathrm{Nu}_s = 0.019\mathrm{Re}_s^{0.817}\mathrm{Pr}^{0.4} \tag{20}$$

$$f_s = 0.211\mathrm{Re}_s^{-0.21} \tag{21}$$

5.1.2. Simulation data compared with experimental data

The simulation results of heat transfer and flow resistance of short-length twisted tape with a twist ratio of $y = 4.25$, a rotated angle of $\alpha = 270^\circ$ and a pitch of $l_p = 525$ mm were compared to the experimental results, as shown in Fig. 6. This figure shows that the simulation data are in good agreement with the experimental data and are within ±5.36% deviation for the heat transfer (Nu) and ±7.71% for the friction factor (f). The CFD simulation over predicted the flow resistance for the moderate Reynolds number. The reason for this error can be attributed to the turbulence of the passing fluid just after the inlet. The inlet flow was not fully developed, which results in slightly less flow resistance than the resistance that was obtained from the CFD simulation. However, for higher and lower Reynolds number, the CFD simulation pressure drops could be justified by an error in the flow model that was used in the CFD simulation. The error in the heat transfer (Nu) can be primarily attributed to the difference in the physical properties. From the Figs. 6–3 given in Ref. [18], it can be concluded that the velocity of air heating is lower than the velocity of isothermal flow in the near-wall region as a result of the fact that the air viscosity increases with an increase in temperature. Moreover, the lower heat transfer rate is caused by the lower velocity gradient in the near-wall region. Therefore, the Nusselt numbers obtained from CFD simulation are higher slightly than the experimental data in this study because of an assumption that the air physical properties are independent to the temperature in the CFD modeling.

5.2. Configuration optimization using numerical simulation

To obtain the optimum configuration of regularly spaced short-length twisted tape in a plain tube, a CFD numerical optimization is performed. To maximize the performance of short-length twisted tape, the optimal configuration should be determined by optimizing between the enhancement of heat transfer and the reduction of friction loss. Following from the definition proposed by Gee and Webb [20], the average Nusselt number and 1/3 power of the friction factor are values that represent the thermal performance of an enhanced heat transfer channel, which have been used in many experimental studies [21–23] and are also used in this work. The heat transfer enhancement efficiency η is defined as

$$\eta = \frac{\left(\mathrm{Nu}/\mathrm{Nu}_{\mathrm{ref}}\right)}{\left(f/f_{\mathrm{ref}}\right)^{1/3}} \tag{22}$$

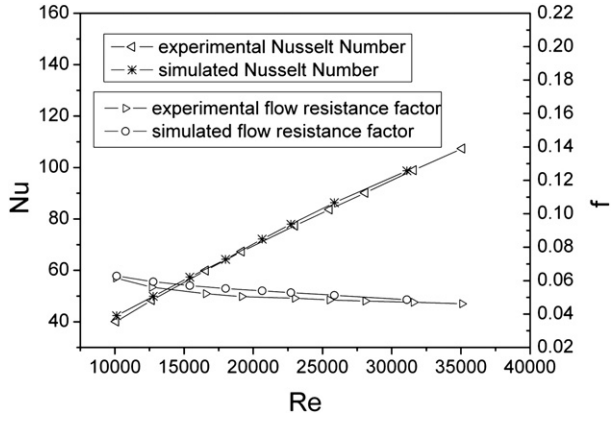

Fig. 6. Comparison of the numerical and experimental results.

5.2.1. Minimum rotated angle at a constant twist ratio

The twisted tape in the tube is more likely to be used in the case of low Reynolds number than in the case of high Reynolds number due to a large pressure drop in the latter. As demonstrated in previous studies, the swirl flow pattern can be induced by twisted tape. Swirl flow can increase the tangential velocity component and can further increase the temperature gradient near the wall. Thus, the heat transfer can effectively be enhanced. Based on this principle, the heat transfer can be enhanced by swirl flow either if it is accompanied by a twisted tape or if it is the free swirl flow generated by an upstream element. Obviously, the latter pattern enhances heat transfer at the cost of a much smaller pressure drop.

To take full advantage of the free swirl flow generated by short-length twisted tape regularly mounted in the tube, the first step of configuration optimization is to determine the minimum rotated angle to reach the maximum distance of the remarkable free swirl flow at a constant twist ratio (e.g., $y = 2.0$). The distance of remarkable free swirl flow downstream of the short-length twisted tape (l_s) can be defined as the distance from the end of short-length twisted tape to its downstream cross-section A–A, as shown in Fig. 1. Furthermore, in the upstream of A–A in the same free space, the velocity magnitude in the core is lower than that in its near region. However, the velocity magnitude of the core in the downstream of A–A within the same free space is higher than that in its near region.

The value of l_s is significantly influenced by the rotated angle of the short-length twisted tape for periodical flow. There exists a minimum value of the rotated angle ($\alpha_{\min}$) for a constant twist ratio that reaches the maximum value of l_s. In other words, if the rotated angle α is larger than $\alpha_{\min}$, then the value of l_s cannot be longer for a constant twist ratio. In this study, a CFD simulation was performed to determine l_s with variations in the rotated angle under the conditions of $d_i = 16$ mm, $\sigma = 1.2$ mm, $l_p = 1000$ mm, $y = 2.0$ and Re = 10,000. Here, l_p is long enough to allow free swirl flow to fully develop, and 10,000 is a commonly used Reynolds number for turbulent flow in practical applications. The variation of l_s with the rotated angle α is illustrated in Fig. 7. The minimum value of the rotated angle is 360°, i.e., a rotated angle larger than 360° cannot lead to a longer distance of free swirl flow for a constant twist ratio ($y = 2.0$).

5.2.2. Optimal twist ratio and rotated angle

To take advantage of the free swirl flow generated by the short-length twisted tape to increase the heat transfer enhancement efficiency, the pitch of the twisted tape elements was assumed to be 600 mm, and the rotated angle was not more than 360° in the optimization modeling of the twist ratio and the rotated angle. Only multiples of 90° were considered for the rotated angle. The rotated angle 90° was excluded from the optimization modeling because it cannot generate typical swirl flow in the tube for turbulent flow.

The variation in the Nusselt number with the twist ratio for $\alpha = 180^\circ$, 270° and 360° is presented in Fig. 8. In this figure, the Nusselt number decreases slightly with an increase in the twist ratio (y), except for a large rotated angle and a high Reynolds number (e.g., $\alpha = 360^\circ$ and Re = 20,000), which can be attributed to a higher turbulent intensity and a stronger mixing of fluid between the near-wall region and the core region with a lower twist ratio. As expected, the Nusselt number increases with an increase in the Reynolds number for all of the cases, and the smallest rotated angle yields the lowest heat transfer rate at a constant twist ratio.

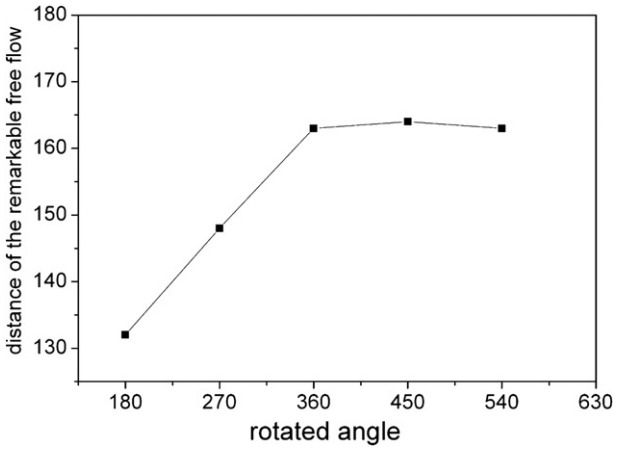

Fig. 7. Relationship of the distance of remarkable free swirl flow to the rotated angle.

The variation in the flow resistance factor with the twist ratio for $\alpha = 180°$, 270° and 360° is shown in Fig. 9. As shown in the figure, the use of a larger rotated angle yields a higher flow resistance for the same twist ratio and a constant Reynolds number. However, the flow resistance factor decreases with an increase in the Reynolds number for all of the short-length twisted tape conditions. In addition, the results demonstrate that, initially, the flow resistance factor decreases significantly as the twist ratio increases, and then it increases slightly with an increase in the twist ratio. In other words, there is a minimum resistance factor over the wide range of twist ratios from 2.5 to 8.0 at a constant rotated angle. This interesting phenomenon could be caused by the turning point of dominant contribution to the total resistance from form resistance to frictional resistance over the wide range of twist ratios from 2.5 to 8.0. Based on the relationship between the length of the twisted tape and its twist ratios ($l = H \cdot \alpha/180 = y \cdot d_i \cdot \alpha/180$), the short-length twisted tape with a higher twist ratio is longer than that with a lower twist ratio for a constant rotated angle. A longer tape results in a larger average frictional resistance for a constant pitch. The total resistance consists of the fraction resistance and the form resistance. For a twist ratio ranging from 8 to 5.75, the frictional resistance decreases, and the form resistance increases along with a decrease in the twist ratio. And what's more, the frictional resistance dominates in the total resistance. Thus, the decrease of frictional resistance is larger than the increase of the form resistance with a decrease of twist ratio. As a result, the total resistance decreases with a decrease of twist ratio from 8 to 5.75. However, over the range of twist ratios from 4.75 to 2.5, the form resistance dominates in the total resistance. Also, the form resistance increases significantly and more rapidly than the decrease in the frictional resistance with a decrease of twist ratio. Therefore, the total resistance increases with a decrease in the twist ratio from 4.75 to 2.5. Regarding the resistance factor across a range of twist ratios ($y = 2.5–8$), it is obvious that the minimum resistance factor occurs when the twist ratio is in the range of 4.75–5.75 with Reynolds numbers ranging from 10,000–20,200.

The variations of the heat transfer enhancement efficiency η with a twist ratio at constant rotated angles ($\alpha = 180°$, 270° and 360°) are shown in Fig. 10. In this figure, the enhancement efficiency η increases rapidly at the beginning and then decreases slowly with an increase in the twist ratio. This variation pattern of enhancement efficiency is primarily attributed to the effects of variation patterns in the flow resistance. The optimal twist ratio is 4.25–4.75 for $\alpha = 180°$, 270° and 360° with Reynolds numbers ranging from 10,000–20,200. A lower Reynolds number corresponds to the higher heat transfer enhancement efficiency. The heat transfer enhancement efficiency for $\alpha = 180°$ is slightly higher than that of

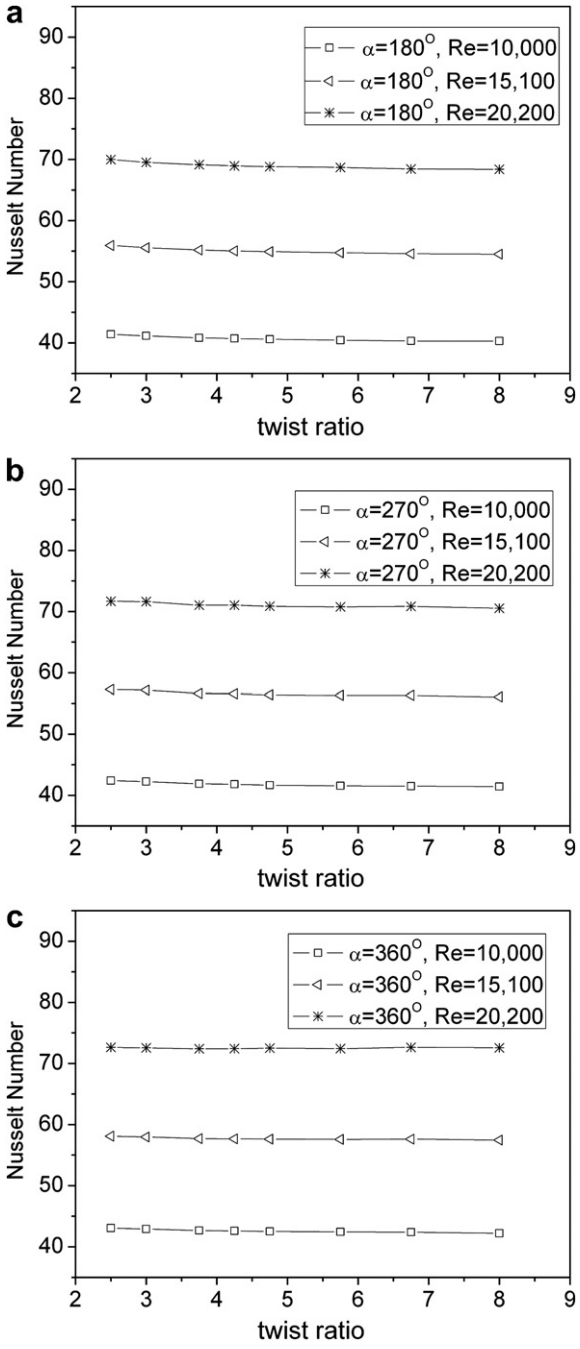

Fig. 8. Variation in the Nusselt number with the twist ratio. (a) Rotated angle is 180°; (b) rotated angle is 270°; (c) rotated angle is 360°.

$\alpha = 270°$; however, the heat transfer enhancement efficiency of $\alpha = 360°$ is significantly lower. Therefore, the optimal rotated angle is 180° for Reynolds numbers ranging from 10,000–20,200, and the maximum enhancement efficiency reaches 1.079. If the heat transfer rate is more important, a rotated angle of $\alpha = 270°$ can be can be used as a reference for industrial application. According to the Fig. 10, the enhancement efficiencies are all higher than 1.0 when $180° \le \alpha \le 270°$, $3.0 \le y \le 8.0$ and $10{,}000 \le \mathrm{Re} \le 20{,}200$.

5.2.3. Optimal free space ratio

If the free space between the short-length twisted tapes is too large, then the distance of remarkable free swirl flow is much shorter than the length of the free space. Thus, the heat transfer of

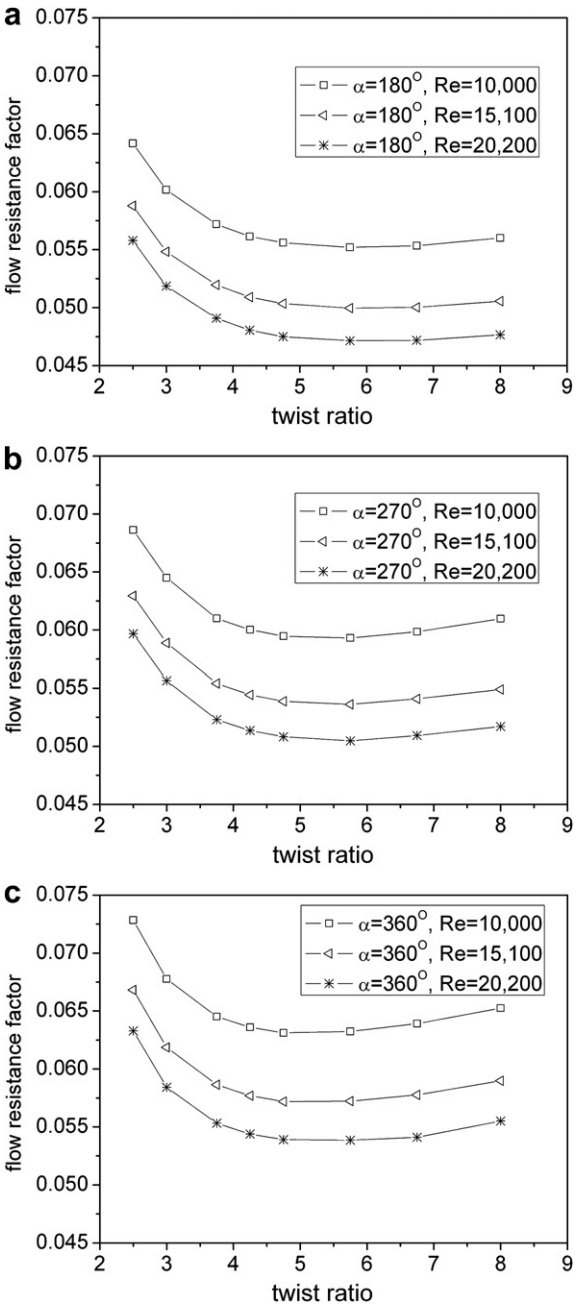

Fig. 9. Variation in the flow resistance factor with twist ratio. (a) Rotated angle is 180°; (b) rotated is 270°; (c) rotated is 360°.

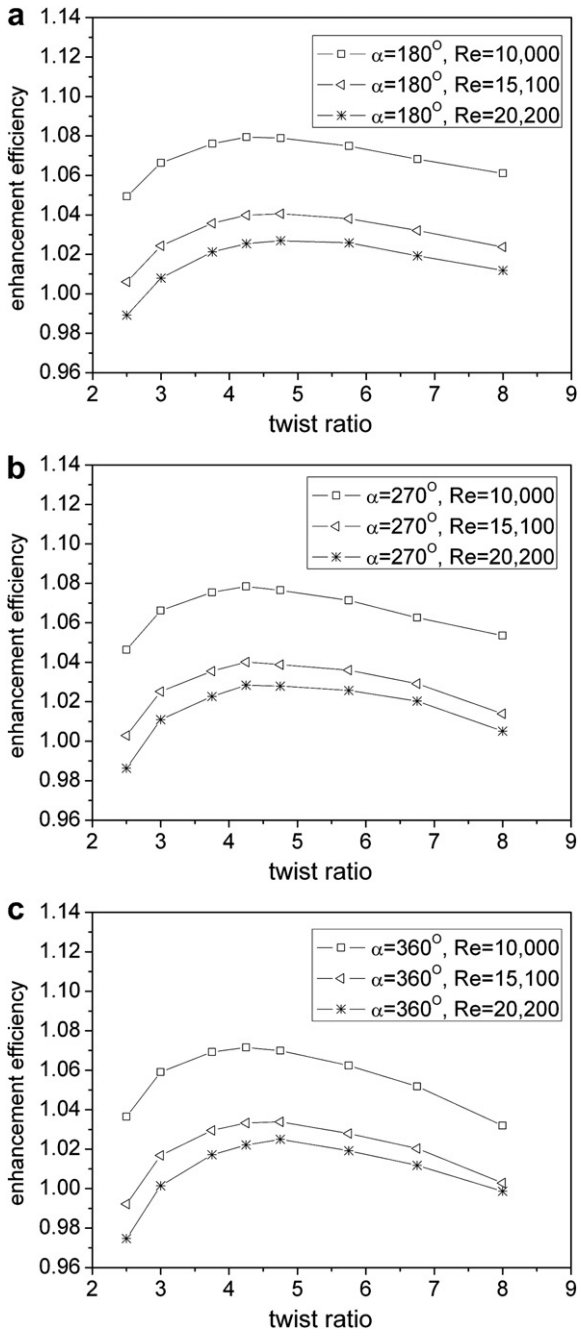

Fig. 10. Variation in the enhancement efficiency with the twist ratio. (a) Rotated angle is 180°; (b) Rotated angle is 270°; (c) Rotated angle is 360°.

the free space without swirling flow between the short-length twisted tapes is not enhanced, which reduces the overall effect of heat transfer enhancement by swirl flow for the equipment. However, if the free space between the short-length twisted tapes is too small, then there is not enough distance for swirl flow to decay, and the swirl flow intensity will still be strong when it reaches the next twisted tape and will build up another swirl flow. In other words, the heat transfer enhancement of the swirl flow is far from being completely exploited. Therefore, there must be an optimal free space ratio.

Due to the large error in the heat transfer caused by the difference in the physical properties between different cases for a wide range of free space ratios, the enhancement efficiency (η) is not a suitable evaluation factor to develop the optimal free space ratio. Hence, the optimal free space ratio should be developed using another method such as the swirl flow evolution process that is presented in this study.

The degree of swirl for a swirling flow can be characterized by the swirl number S [24], which is defined as $S = \int_0^A \rho u_y u_\theta r dA / \frac{d_i}{2} \int_0^A \rho u_y^2 dA$. The swirl number is a ratio of the axial flux of angular momentum to the axial flux of axial momentum. The variation in the swirl number with the y coordinate at a constant twist ratio ($y = 4.25$) for various rotated angles ($\alpha = 180°, 270°$) is shown in Fig. 11. In this figure, the swirl flow is quickly enhanced by the short-length twisted tape and then decays gradually downstream until the next one is built up again. The use of a larger free space ratio yields a weaker swirl flow; subsequently, the effect on heat transfer and flow resistance by the short-length twisted tape is reduced. The axial velocity

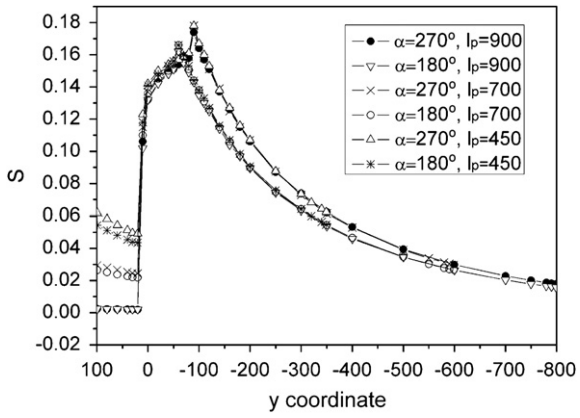

Fig. 11. Variation in the swirl number with the y coordinate.

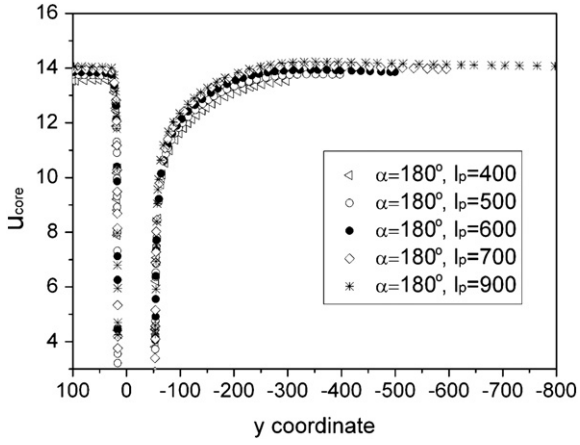

Fig. 12. Variation in the velocity magnitude in core with the y coordinate (rotated angle is 180°).

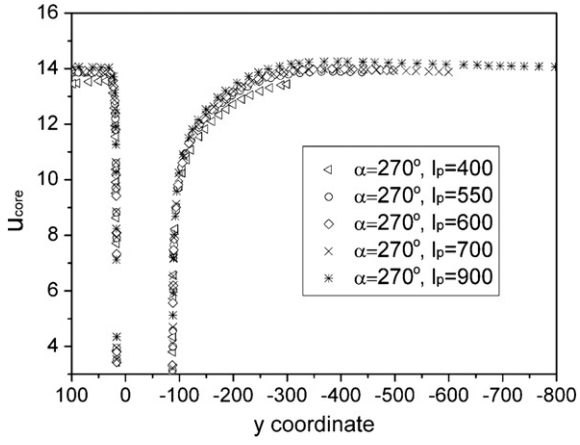

Fig. 13. Variation in the velocity magnitude in core with the y coordinate (rotated angle is 270°).

magnitude in the core of the tube with the y coordinate at a constant twist ratio ($y = 4.25$) for $\alpha = 180°$, 270° is shown in Fig. 12 and Fig. 13, respectively. Along with swirl flow decay, the axial velocity magnitude increases until the swirl flow disappears. From Figs. 11–13, the optimal pitch of every two consecutive short-length twisted tape should be in the range of 550–600 mm, and the corresponding optimal free space ratio (s) is in the range of 28–33 for short-length twisted tape with $\alpha = 270°$ or $\alpha = 180°$ at $y = 4.25$ for Reynolds numbers ranging from 10,000–20,200.

6. Conclusions

The configuration optimization of regularly spaced short-length twisted tape in a circular tube for turbulent flow was performed using a CFD simulation based on heat transfer enhancement efficiency. The following conclusions can be drawn from the present study.

1) The twist ratio (y) is a critical factor that influences the flow resistance characteristic for short-length twisted tape regularly spaced in a circular tube. Additionally, there is a minimum resistance factor over a wide range of twist ratios from 2.5 to 8.0 for a constant rotated angle and pitch, which can be attributed to the turning point of dominant contribution to the total resistance from form resistance to frictional resistance over the wide range of twist ratios from 2.5 to 8.0. Over the range of twist ratios from 2.5 to 4.75, the form resistance dominates the total resistance and increases significantly and more rapidly compared to the decrease in the frictional resistance along with a decrease of twist ratio. As a result, the overall flow resistance decreases with an increase of twist ratio in the range of 2.5–4.75. Whereas, when twist ratio is in the range of 5.75–8.0, the frictional resistance dominates the overall resistance and increases significantly and more rapidly compared to the decrease in the form resistance along with an increase of twist ratio. Thus, the overall flow resistance increases along with an increase of twist ratio in the range of 5.75–8.0. The minimum resistance factor occurs when the twist ratio is in the range of 4.75–5.75 with Reynolds numbers ranging from 10,000 to 20,200.
2) A smaller twist ratio (y) results in better heat transfer performance with the twist ratio varying from 2.5 to 8.0, except for large rotated angles and a high Reynolds number (e.g., $\alpha = 360°$ and Re = 20,200).
3) Both the mean heat transfer and flow resistance increase with an increase in the rotated angle (α). Whereas, a larger free space ratio (s) is related to a weaker effect on the heat transfer and flow resistance from the short-length twisted tape.
4) The optimal design of regularly spaced short-length twisted tape in a circular tube for turbulent air flow based on heat transfer enhancement efficiency (η) is a twist ratio of $y = 4.25$–4.75, a rotated angle of $\alpha = 180°$ and a free space ratio of $s = 28$–33 for Reynolds numbers varying from 10,000 to 20,200. If the heat transfer rate is more important, the second design of $y = 4.25$–4.75, $\alpha = 270°$ and $s = 28$–33 in the range of Reynolds numbers from 10,000 to 20,200 can be used as a reference for industrial application.
5) When $s = 28$–33, $180° \leq \alpha \leq 270°$, $3.0 \leq y \leq 8.0$ and $10{,}000 \leq Re \leq 20{,}200$, the enhancement efficiency is higher than 1.0. The maximum enhancement efficiency is 1.079.

Acknowledgements

This work was supported by the Shanghai Leading Academic Discipline Project (No. S30109), the National Natural Science Foundation of China (No. 10772110) and "SEC E-Institute: Shanghai High Institutions Grid" projects.

Nomenclature

H	pitch for 180° rotation of the short-length twisted tape (mm)
l_p	pitch of every two consecutive short-length twisted tape (mm)
l	length of the short-length twisted tape (mm)

l_s	maximum distance of the free swirl flow (mm)
$l_{\exp}$	length of the test tube in the experiment (mm)
d	diameter(m)
y	twist ratio
s	free space ratio
S	swirl number
x, y, z	Cartesian coordinate system
Q	heat transfer rate (W)
$\dot{m}$	mass flow rate of air (kg s^{-1})
C_p	specific heat (J kg^{-1} K^{-1})
t	temperature (K)
V	volume flow rate of air (m^3 h^{-1})
U	averaged axial velocity inside of the test section (m s^{-1})
u	velocity magnitude (m s^{-1})
Nu	averaged Nusselt number
Pr	fluid Prandtl number
Re	Reynolds number
P	static pressure (Pa)
ΔP	pressure drop (Pa)
f	flow resistance factor
h	heat transfer coefficient (W m^{-2} K^{-1})
K	overall heat transfer coefficient (W m^{-2} K^{-1})
$\vec{u}$	velocity vector (m s^{-1})
e	total energy (J)
g	gravitational acceleration (m s^{-2})
∇T_m	logarithmic mean temperature difference (K)
R	thermal resistance (m^2 K J^{-1})

Greek symbols

α	rotated angle (°)
δ	thickness of the short-length twisted tape (mm)
μ	dynamic viscosity of the working fluid (kg/ms)
μ_T, μ_{eff}	turbulent and effective viscosity (kg/ms)
$\bar{\bar{\tau}}_{eff}$	stress tensor (kg/ms^2)
ρ	air density (kg/m^3)
λ	thermal conductivity (W/mK)
η	heat transfer enhancement efficiency

Subscripts

a	air
ave	average
c	cold
h	hot
i	inside
o	outside
in	inlet
out	outlet
w	wall
steam	steam
ref	reference value
m	logarithmic mean temperature
s	plain tube without twisted tape insert
θ	tangential direction
y	y-coordinate direction
x	x-coordinate direction
core	core of the tube

References

[1] S. Garimella, R.N. Christensen, Heat transfer and pressure drop characteristics of spirally fluted annuli: part I-hydrodynamics, ASME Journal of Heat Transfer 117 (1995) 54–60.

[2] A.E. Bergles, Augmentation of forced-convection heat transfer. in: S. Kakac, D.B. Spalding (Eds.), Turbulent Forced Convection in Channels and Bundles. Hemisphere Publishing Co, Washington, DC, 1973, pp. 883–909.

[3] P. Promvonge, S. Eiamsa-ard, Heat transfer enhancement in a tube with combined conical-nozzle inserts and swirl generator, Energy Conversion and Management 47 (2006) 2867–2882.

[4] P. Promvonge, S. Eiamsa-ard, Heat transfer augmentation in a round tube using V-nozzle turbulator inserts and snail entry, Experimental Thermal and Fluid Science 32 (2007) 332–340.

[5] S.W. Hong, A.E. Bergles, Augmentation of laminar flow heat transfer in tubes by means of twisted-tape inserts, ASME Journal of Heat Transfer 98 (1976) 215–256.

[6] W.J. Marner, A.E. Bergles, Augmentation of highly viscous laminar heat transfer inside tube in constant wall temperature, Experimental Thermal and Fluid Science 2 (1989) 252–267.

[7] R.M. Manglik, A.E. Bergles, Laminar flow heat transfer in a semi-round tube with uniform wall temperature, International Journal of Heat and Mass Transfer 31 (1988) 625–636.

[8] R.M. Manglik, A.E. Bergles, Heat transfer and pressure drop correlations for twisted-tape inserts in isothermal tubes: part II-transition and turbulent flows, ASME Journal of Heat Transfer 115 (1993) 890–896.

[9] P.K. Sarma, P.S. Kishore, R.V. Dharma, T. Subrahmanyam, A combined approach to predict friction coefficients and convective heat transfer characteristics in a tube with twisted tape inserts for a wide rang of Re and Pr, International Journal of Thermal Sciences 44 (2005) 393–398.

[10] S.W. Chang, Y.J. Jan, J.S. Liou, Turbulent heat transfer and pressure drop in tube fitted with serrated twisted-tape, International Journal Thermal Sciences 46 (2007) 506–518.

[11] S.K. Saha, U.N. Gaitonde, A.W. Date, Heat transfer and pressure drop characteristics of laminar flow in a circular tube fitted with regularly spaced twisted-tape elements, Experimental Thermal and Fluid Science 2 (1989) 310–322.

[12] A.W. Date, U.N. Gaitonde, Development of correlations for predicting characteristics of laminar flow in a tube fitted with regularly spaced twisted-tape elements, Experimental Thermal and Fluid Science 3 (1990) 373–382.

[13] A.W. Date, S.K. Saha, Numerical prediction of laminar flow and heat transfer characteristics in a tube fitted with regularly spaced twisted-tape elements, International Journal of Heat and Fluid Flow 11 (1990) 346–354.

[14] S.K. Saha, A. Dutta, S.K. Dhal, Friction and heat transfer characteristics of laminar swirl flow through a round tube fitted with regularly spaced twisted-tape elements, International Journal of Heat and Mass Transfer 44 (2001) 4211–4223.

[15] Smith Eiamsa-ard, Chinaruk Tianpong, Petpices Eiamsa-ard, Pongjet Promvong, Convective heat transfer in a circular tube with short-length twisted tape insert, International Communications in Heat and Mass Transfer 36 (2009) 365–371.

[16] S. Eiamsa-ard, C. Thianpong, P. Promvonge, Experimental investigation of heat transfer and flow friction in a round tube fitted with regularly spaced twisted tape elements, International Communications in Heat and Mass Transfer 33 (2006) 1225–1233.

[17] T.-H. Shih, W.W. Liou, A. Shabbir, Z. Yang, J. Zhu, A new k–ϵ eddy viscosity model for high Reynolds number turbulent flows-model development and validation, Computers Fluids 24 (1995) 227–238.

[18] J.P. Holman, Heat Transfer, ninth ed. McGraw-Hill Higher Education, 2002.

[19] F.P. Incropera, P.D. Witt, T.L. Bergman, A.S. Lavine, Fundamentals of Heat and Mass Transfer. John-Wiley & Sons, 2006.

[20] D.L. Gee, R.L. Webb, Forced convection heat transfer in helically rib-roughened tubes, International Journal of Heat and Mass Transfer 23 (1980) 1127–1136.

[21] J.C. Han, J.S. Park, C.K. Lei, Heat transfer enhancement in channels with turbulence promoters, Journal of Engineering for Gas Turbines and Power 107 (1985) 628–635.

[22] H.H. Cho, S.Y. Lee, S.J. Wu, The combined effects of rib arrangements and discrete ribs on local heat/mass transfer in a square duct, ASME 2001-GT-0175 (2001).

[23] M.E. Taslim, C.M. Wadsworth, An experimental investigation of the rib surface-averaged heat transfer coefficient in a rib roughened square passage, Journal of Turbomachinery 119 (1997) 381–389.

[24] Weizao Gu, Chongfang Ma, Heat Transfer Enhancement. Science Press, China, 1991.